

Sintering effects on the hardness of β -tricalcium phosphate

Behzad Mehdikhani^{a,*}, Bahman Mirhadi^b and Nayereh Askari^a

^aStandard Research Institute, Ceramic Department, Karaj, Iran

^bImam Khomeini International University, Engineering Department, Qavin, Iran

Nano-size β -tricalcium phosphate (β -TCP) powders with an average grain size of 70-100 nm were prepared by the wet chemical precipitation method with calcium nitrate and di-ammonium hydrogen phosphate as calcium and phosphorus precursors, respectively. The precipitation process employed was also found to be suitable for the production of sub-micrometre β -TCP powder in situ. The sinterability of the nano-size powders, and the microstructure, mechanical strength of the β -TCP bioceramics prepared were investigated. Bioceramic sample characterization was achieved by powder X-ray diffraction (XRD), scanning electron microscopy (SEM), Fourier transform infrared spectroscopy (FTIR) and density measurements. Powders compacted and sintered at 800, 900, 1000 and 1100 °C showed an increase in relative density from 68% to 93%. The results revealed that the maximum hardness of 240 H_V was obtained for β -TCP sintered at 1100 °C.

Key words: Beta tricalcium phosphate, Bioceramic, Sintering, Mechanical properties.

Introduction

Calcium phosphate bioceramics are materials of choice for bone tissue repair because of their similarity of composition with bone mineral; excellent bioactivity; ability to promote cellular expressions; and osteoconductivity [1-3]. The calcination constitutes a necessary step of the preparation when wet chemical routes are used for the synthesis of calcium phosphate, i.e. precipitation from the neutralization of Ca(OH)₂ with H₃PO₄ or from the decomposition of Ca(NO₃)₂ and (NH₄)₂HPO₄. Moreover, an analysis of particle growth during calcination is required to understanding of grain growth phenomena that occur during the final stages of the densification [4]. β -TCP ceramic is known as β -whitlockite and is a slow degrading resorbable phase [5] and is thus a promising material in biomedical applications. β -TCP is known to have significant biological affinity, activity and hence responds well to physiological environments [6]. Because of these positive characteristics, porous β -TCP is regarded as an ideal bone substitute, which would degrade in vivo with time allowing bone tissue to grow inside the scaffold [7]. TCP has three polymorphs, β -TCP is stable below 1180 °C, α -TCP between 1180 °C and 1400 °C, and α' -TCP above 1470 °C. Among the three allotropic forms, β -TCP is preferred as a bioceramic on account of its chemical stability, mechanical strength, and proper bioresorption

rate. To use β -TCP ceramics as surgical implants, the mechanical strength of β -TCP ceramics must be as high as possible. The density of β -TCP ceramics is also an important factor. Generally, it is difficult to sinter β -TCP ceramics fully because β -TCP ceramics should be sintered at a lower temperature than that of the phase transition to α -TCP [8]. TCP is a resorbable temporary bone space filler material. When implanted, TCP will interact with body fluids and form HA in accordance to the following equation:



Theoretically, resorbable TCP is an ideal implant material. After implantation, TCP will degrade with time and be replaced with natural tissues. This leads to the regeneration of tissues instead of their replacement and so solves the problem of interfacial stability [9, 10]. β -TCP powders are reportedly prepared by liquid-solution methods, such as sol-gel, hydrothermal, micro emulsion and precipitation, as well as gas phase reactions [11-13]. β -TCP is routinely used as a bone replacement, especially in the field of oral and craniofacial surgery, in the form of granules and rods [14, 15] or as filler in polymeric scaffolds [16]. In the bulk, β -TCP bioceramics have mechanical properties too poor to be used in load-bearing clinical applications [17-19], which has been attributed to the difficulties in fully densifying β -TCP powders [18, 20-22]. These difficulties are associated with the presumption that the sintering temperature should be kept below 1125 °C to avoid the $\beta \rightarrow \alpha$ phase transformation that is considered deleterious to

*Corresponding author:
Tel : 00989126417516
Fax: 00982413230496
E-mail: mehdikhani@standard.ac.ir

mechanical properties. Material properties deemed particularly important when designing calcium phosphates with improved resorption are surface characteristics, such as: roughness, grain size and porosity, and chemical properties, in particular phase composition. It is possible to use different sintering regimes to change the surface roughness, grain size and density for example by using high and low temperatures [23], however the use of high sintering temperatures causes unwanted phase changes to occur (e.g. β -TCP to α -TCP) [24]. One of the critical controlling parameter that requires attention during the processing of β -TCP is the selection of a suitable sintering method to obtain a solid and high density β -TCP body that is characterized by having a fine-grained microstructure [25]. Dense nano structured bioceramic materials are usually obtained by pressing and conventional sintering of nanopowders using pressure assisted methods, such as hot pressing, hot isostatic pressing, sinter forging, etc [26-28]. The high sintering temperatures and long sintering times required for the consolidation of β -TCP powders often result in extreme grain coarsening and decomposition of the β -TCP, which is a characteristic for the conventional sintering methods and results in the deterioration of the mechanical properties of β -TCP ceramics [29, 30]. The aim of this study was to determine the effects of the sintering temperature on the microstructure and mechanical properties of β -TCP scaffolds by means of nanoindentation testing. In this study, β -TCP scaffolds were manufactured through a wet chemical precipitation process and subsequently sintered at four different temperatures. Scaffolds were characterized in terms of their crystallographic phases, microstructural morphology, grain size, density and hardness.

Experimental Procedure

Powder synthesis

The precipitation procedures that were used in the synthesis of β -TCP pure bioceramic powders are described in detail in the process flowchart given in Fig. 1. β -TCP nanopowders were synthesized by the reaction of calcium nitrate tetra-hydrate ($\text{Ca}(\text{NO}_3)_2 \times 4\text{H}_2\text{O}$, 98%, Merck) with diammonium hydrogen phosphate ($(\text{NH}_4)_2\text{HPO}_4$, 99%, Merck). Briefly, 500 ml of 0.4 mol $(\text{NH}_4)_2\text{HPO}_4$ solution with a pH = 4 was vigorously stirred at room temperature, and 500 ml of 0.6 mol $\text{Ca}(\text{NO}_3)_2$ with a pH = 7.3 was added drop wise over 150-200 minute to produce a white precipitate. Throughout the mixing process the pH of the system was maintained at pH = 8 by adding of 0.1 M sodium hydroxide (NaOH, 99%, Merck). The white suspension obtained was then stirred for 12 h. The synthesized precipitate was washed with distilled water and then with 100% ethanol to improve the dispersion characteristics. The suspension was filtered in a filter

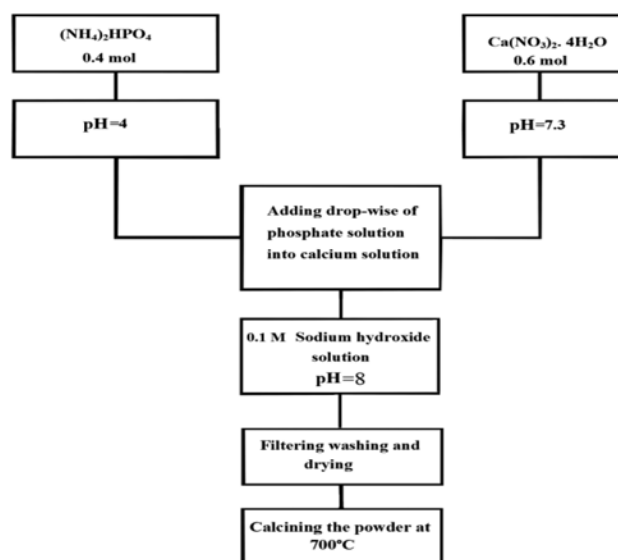


Fig. 1. Chemical precipitation flowchart used in the synthesis of β -TCP pure nanobioceramic powders.

glass with application of mild suction. After filtration the compact, sticky filter cake, was dried at 80 °C for 24 h. The as-dried powders were crushed by using a mortar and pestle and calcined in an alumina crucible at 700 °C for 2 h. The synthesized β -TCP powder was isostatically pressed at 50 MPa, for 1 minute, resulting in uniform green compacts, which were sintered at temperatures from 800, 900, 1000 and 1100 °C in an air atmosphere for 6 h. The initial heating rate was 20 °K.minute⁻¹. The β -TCP compact density was measured using Archimedes' method. The sintered β -TCP compacts were tested for microhardness. Microhardness was measured with a Vicker's indenter. Samples were embedded in epoxy and surfaces were ground flat and polished to a 1 μm finish with diamond paste. Each sample was indented 10 times with 200 g and 300 g loads. No effect of load on hardness values was noticed at these loads.

Characterization of β -TCP bioceramic powders

Evaluation of crystalline phases was investigated by X-ray diffractometer (Siemens, model D-500) using $\text{CuK}\alpha$ radiation. Silicon powder was used as the standard material for semi-quantitative analysis of the precipitated phases. The mean crystallite size (D) was calculated from XRD line broadening measurements from the Scherrer equation [31]:

$$D = 0.89\lambda / \beta \cos\theta \quad (2)$$

where λ is the wavelength of the Cu $\text{K}\alpha$ radiation used, β is the full width at the half maximum of the β -TCP line and θ is the diffraction angle. Infrared spectra were performed by FTIR Bomem (model MB100, Quebec, Canada) in the 400-4000 cm^{-1} wavenumber region. For infrared spectroscopy, samples were pulverized and mixed with a given amount of potassium bromide (KBr)

and pressed into very thin tablets. The Ca/P ratio of the dried powder was measured by inductively coupled plasma (ICP) atomic emission spectroscopy (model Varian). Powder morphology and particle size were evaluated using a scanning electron microscope (SEM, VEGA-TESCAN).

Results and Discussion

The morphology of the TCP powder precipitated is shown in Fig. 2. It can be seen that the β -TCP powder is highly agglomerated with almost spherical particles having an average size of 70-100 nm. The Ca/P ratio of the β -TCP powder, as determined by ICP analyses, was 1.51 ± 0.01 . The XRD analysis was performed using the X-ray diffractometer. The straight base line and sharp peaks of the diffractogram in Fig. 3 confirmed that the products were well crystallized. The results revealed that the as-prepared powder was highly crystalline β -TCP with no second phase. The average crystallite size was determined by the Scherrer equation, of this sample was 80 nm. In order to identify the molecular arrangement of the precipitated powders, FT-IR analysis was performed. The FTIR spectrum of

the powder is shown in Fig. 4. The characteristic absorption bands at 3433 and 1631 cm^{-1} are attributed to adsorbed water. The bands at 900-1200 cm^{-1} were the stretching mode of the PO_4^{3-} group. The sharp peaks at 561 and 607 cm^{-1} represent the vibration peaks of PO_4^{3-} in the β -TCP [32-33]. A SEM micrograph of the green compact isostatically pressed at 50 MPa is shown in Fig. 5. The compact, as can be clearly seen, was uniform, as the result of the applied high isostatic pressure and the presence of soft aggregates in the starting β -TCP powder. The green compacts of β -TCP were sintered in air to obtain compacts having a dense microstructure. The green compact density was 1.36 g/cm^3 , or 60.4% of the theoretical density. Fig. 6 shows the relative density of samples sintered from nano-size powders as a function of the sintering temperature. The density of samples increased up to 1100 $^\circ\text{C}$. The hardness of samples increased with the sintering temperature and reached a maximum at 1100 $^\circ\text{C}$. The density could be seen to increase with increasing

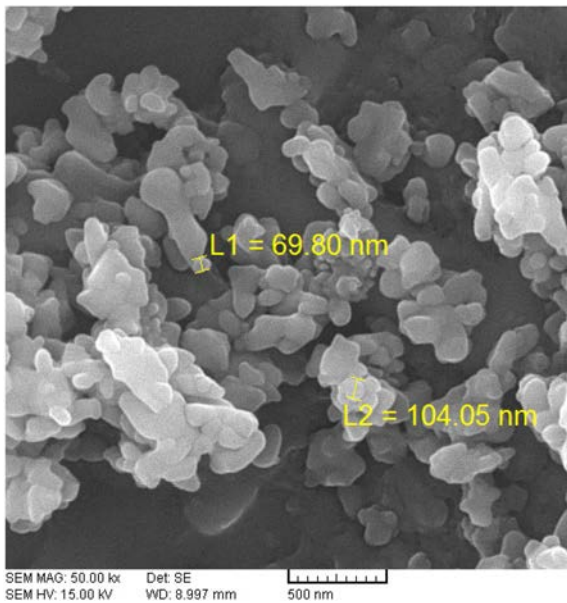


Fig. 2. SEM photomicrograph of the prepared β -TCP nanopowders.

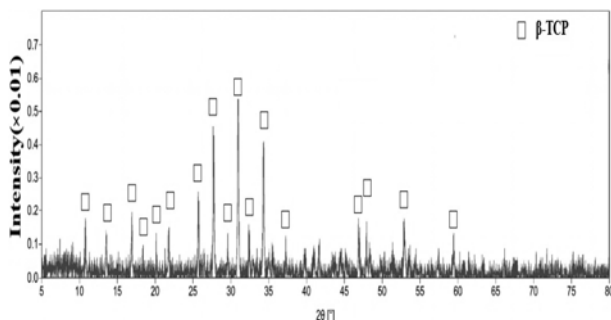


Fig. 3. XRD pattern of the β -TCP powders.

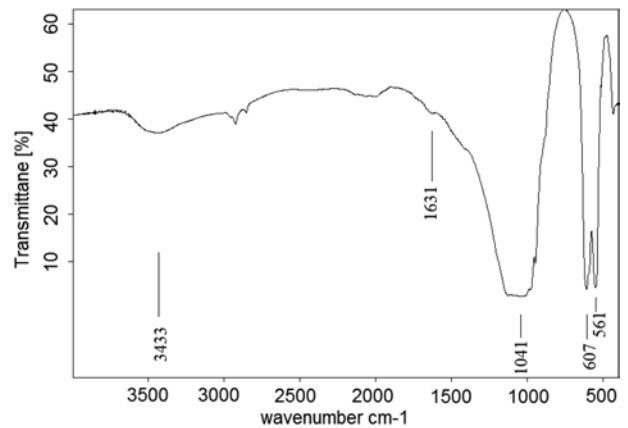


Fig. 4. FTIR spectrum of β -TCP.

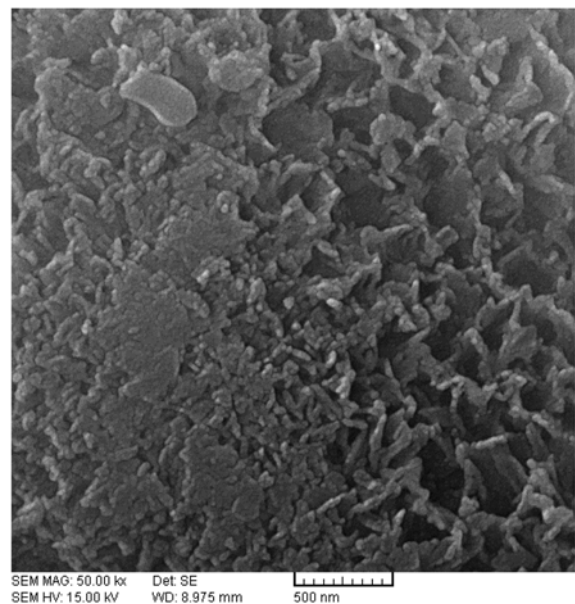


Fig. 5. Typical SEM micrograph of a green compact of β -TCP powder pressed at 50 MPa.

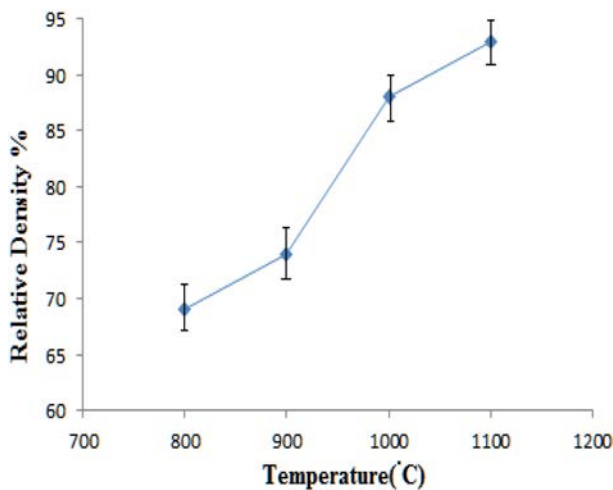


Fig. 6. Relative density of β -TCP bioceramics fabricated from nano-size powders.

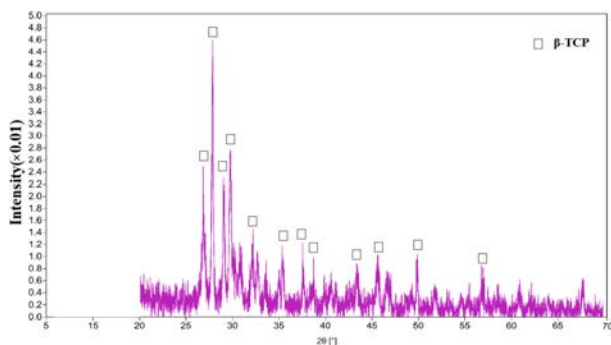


Fig. 7. XRD pattern of the β -TCP bioceramics prepared using nano-size powders: sintered at 1100 °C.

sintering temperature. When sintered at 800 °C, the relative density (RD) of the β -TCP powders only reached 68%. With an increase of the sintering temperature to 900 and 1000 °C, the relative density increased to 74% and 87%. With a further increase in the temperature, the (RD) increased sharply, and reached 93% at 1100 °C. Fig. 7 shows the XRD pattern of the sample sintered at 1100 °C. It can be seen that the sample was composed of highly crystalline and single-phase β -TCP, and no other phases were observed. SEM micrograph of the fracture surface of samples obtained by sintering at 800- 1100 °C for 6 h is shown in Fig. 8. Fig. 8-a shows that spherical agglomerates of crystals are approximately 100 nm in diameter. A fracture surface of the sample fired at 900 °C is shown in Fig. 8-b. The highly reactive spherical particles in the sample were joined by neck growth and a continuous pore channel was formed, as is clearly seen in the micrograph. The particles in the sample fired at 900 °C have lost their identity and considerable grain growth has occurred; the sample appears to be in the intermediate stage of sintering and the particles were approximately cylindrical with dimensions $1 \mu\text{m} \times 0.25 \mu\text{m}$. The fracture surface of a sample sintered at 1000 °C, is shown in Fig. 8-c. Grain

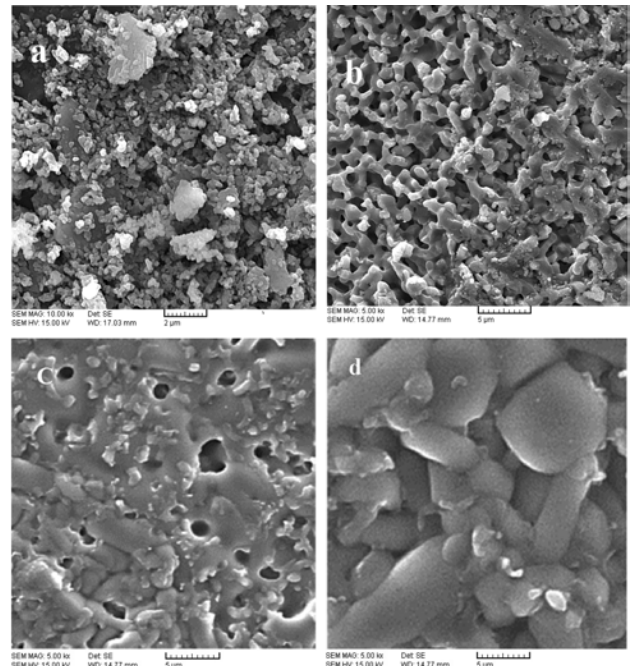


Fig. 8. SEM micrographs of β -TCP powders sintered at various temperatures in air for 6 h after being uniaxially pressed at 50 MPa: (a) 800 °C; (b) 900 °C; (c) 1000 °C; (d) 1100 °C.

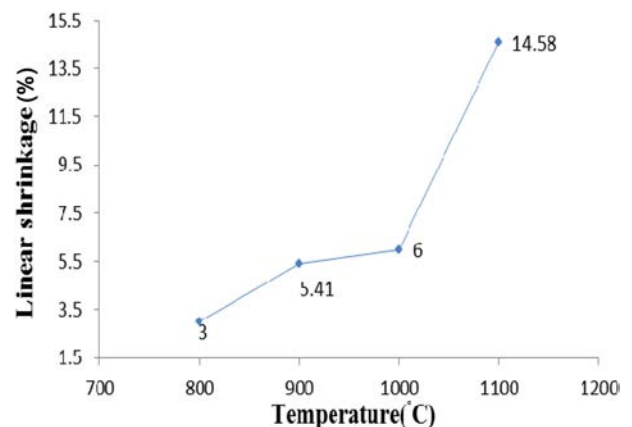


Fig. 9. Linear shrinkage of β -TCP sintered at different temperatures.

boundaries and isolated pores are visible. The average grain size was 1.25 μm . Fig. 8-d shows the fracture surface of a sample sintered at 1100 °C. The porosity was eliminated and the average grain size was 2.5 μm . During the intermediate and final stages of sintering, pore elimination has occurred without considerable grain growth. The linear shrinkage of the samples sintered at 800-1100 °C is shown in Fig. 9. During the process of sintering from 800 °C to 1100 °C, linear shrinkage of the samples has increased. With an increase of the temperature from 800 °C to 1000 °C, the shrinkage of the samples insignificantly increased, but the shrinkage of the sample rapidly increased, from 6.0% to 14% by sintering at 1100 °C. The effect of the sintering temperature on the Vickers hardness of β -TCP sintered at various temperatures is shown in Fig. 10. For the samples fabricated from nano-size β -TCP

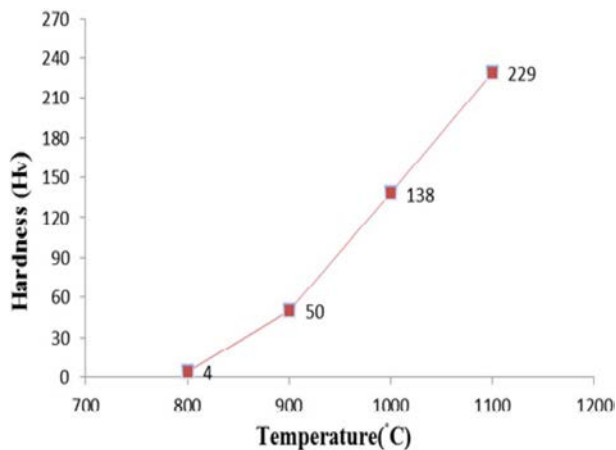


Fig. 10. Vickers hardness of β -TCP sintered at various temperatures.

powders, an increase of the sintering temperature from 800 °C to 1100 °C resulted in an increase of the hardness, which was due to the improved density at the higher sintering temperature.

Conclusion

In this study, the synthesis of biocompatible nano-sized β -TCP powder via a wet precipitation method and using calcium and phosphorous precursors is reported. It is shown that a high purity product, β -TCP nanopowder could be obtained by this simple process. The sample prepared at pH = 8 is β -TCP powder with a Ca/P ratio of 1.51. The sintering ability of the nano-size β -TCP powders, and the microstructure and hardness of the β -TCP bioceramic prepared were investigated. Using nano-size β -TCP powders as raw materials is an effective way to obtain dense ceramic with a high hardness at a 1100 °C sintering temperature.

Acknowledgements

The authors are indebted to the Ceramic Laboratory (Standard research Institute) that supplied the raw materials for development of this research and to the Ceramic Department (International University of Imam khomeini) for its financial support.

References

1. L.L. Hench, *Bioceramics*, J. Am. Ceram. Soc. (81) 1998.
2. A. Ravaglioli, A. Krajewski, *Bioceramics: Materials, Properties and Applications*, Chapman and Hall, London (1992).
3. K.D. Groot, C.P.A.T. Klein, J.G.C. Wolke, J.M.A. Blicck-Hogervorst, *Chemistry of Calcium Phosphate Bioceramics*, in: T. Yamamuro, L.L. Hench, J. Wilson (Eds.), *Handbook of Bioactive Ceramics*, Vol. 2, Calcium Phosphate and Hydroxylapatite Ceramics, CRC Press, Boca Raton, FL (1990) 3-16.
4. D. Bernache-Assollanta, A. Ababoua, E. Championa, M. Heughebaert, *Journal of the European Ceramic Society*. 23 (2003) 229-241.
5. F.C. Driessens, J.W. Van Dijk, J.M. Borggreven, *Calcif. Tissue Res.* 26 (1978) 127.
6. N. Kivrak and A.C. Tas. *J. Am. Ceram. Soc.* 81 (1998) 2245-52.
7. M. Jarcho, R.L. Salisbury, M.B. Thomas, R.H. Doremus, *J. Mater. Sci.* 14 (1979) 142.
8. B. Mirhadi, B. Mehdikhani, N. Askari, *J. Processing and Application of Ceramics*. 5 (2011).
9. K. de Groot, *Ceram. Int.*, 19 (1993) 363-366.
10. S. Metsger, T.D. Driskell, J.R. Paulsrud, *J. Am. Dent. Assoc.* 105 (1982) 1035-1038.
11. K. Lin, J. Chang, J. Lu, W. Wu, Y. Zeng, *J. Ceram. Int.* 33 (2007) 979-985.
12. J.S. Bow, S.C. Liou, S.Y. Chen, *J. Biomater.* 25 (2004) 3155-3161.
13. F. Zhang, K. Lin, J. Chang, J. Lu, C. Ning, *J. Eur. Ceram. Soc.* 28 (2008) 539-545.
14. H.H. Horch, R. Sader, C. Pautke, A. Neff, H. Deppe, A. Kolk., *International Journal of Oral and Maxillofacial Surgery*. 35 [8] (2006) 708-713.
15. U.W. Jung, H.I. Moon, C. Kim, Y.K. Lee, C.K. Kim, S.H. Choi, *J. Current Applied Physics* 5 [5] (2005) 507-511.
16. M. Yoneda, H. Terai, Y. Imai, T. Okada, K. Nozaki, H. Inoue, S. Miyamoto, K. Takaoka, *J. Biomaterials.*, 26 (25), 5145-5152 (2005).
17. M. Sous, R. Bareille, F. Rouais, D. Clement, J. Amedee, B. Dupuy, C. Baquey, *J. Biomaterials*. 19 [23] (1998) 2147-2153.
18. P. Miranda, E. Saiz, K. Gryn, A.P. Tomsia, *J. Acta Biomaterialia*. 2 [4] (2006) 457-466.
19. P. Miranda, A. Pajares, E. Saiz, A.P. Tomsia, F. Guiberteau. *Journal of Biomedical Materials Research Part A*. 85A [1] (2008) 18-227.
20. H.S. Ryu, H.J. Youn, K.S. Hong, B.S. Chang, C.K. Lee, S.S. Chung, *J. Biomaterials*. 23 [3] (2002) 909-914.
21. R. Famery, N. Richard, P. Boch, *J. Ceramics International*. 20 [5] (1994) 327-336.
22. K. Itatani, T. Nishioka, S. Seike, F.S. Howell, A. Kishioka, M. Kinoshita. *Journal of the American Ceramic Society*. 77 [3] (1994) 801-805.
23. Rahaman MN. *Ceramic Processing*. Boca Raton: Taylor & Francis (2007).
24. Huang J, Pan Y, Shao CY. *J. 3 . Sci.* 38 (2003) 1049-56.
25. S. Ramesh, C.Y. Tan, S.B. Bhaduri, W.D. Teng, I. Sopyan. *J. materials processing technology* 206 (2008) 221-230.
26. M.J. Mayo "Nanocrystalline ceramics for structural applications: processing and properties", in: G.M. Chow, N.I. Noskova, *Nanostructured* (Eds.), *Materials Science Technology*, NATO ASI Series, Kluwer Academic Publishers, Russia (1997) 361-385.
27. J.R. Groza, *Nanosintering*, *Nanostruct. Mater.* 12 (1999) 987-992.
28. Dj. Veljovic, B. Jokic, I. Jankovic-Castvan, I. Smiciklas, R. Petrovic, Dj. Janackovic. *J. Key Eng. Mater.* 330 (2007) 259-262.
29. Y.W. Gua, K.A. Khora, P. Cheang, *J. Biomaterials*. 25 (2004) 4127-4134.
30. C.Y. Tang, P.S. Uskokovic, C.P. Tsui, Dj. Veljovic, R. Petrovic, Dj. Janackovic. *J. Ceram. Int.* 35 (2009) 2171-2178.
31. L.A. Azaroff. McGraw-Hill, New York (1968) 38-42.
32. C. Biqin, Z. Zhaoquan, Z. Jingxian, L. Qingling, J. Dongliang. *J. Mater. Sci. Eng. C*. 28 (2008) 1052-1056.
33. S. Raynaud, E. Champion, D. Bernache-Assollant, P. Thomas. *J. Biomater* 23 (2002) 1065-1072.